Inference of Wi-Fi Busy Time Fraction based on Markov Chains

Nour El Houda Bouzouita, Anthony Busson, Hervé Rivano

Inference of Wi-Fi Busy Time Fraction based on Markov Chains

Nour El Houda Bouzouita[a,*], Anthony Busson[a], Herve Rivano[b]

[a] *Univ Lyon, UCBL, EnsL, CNRS, Inria, LIP, F-69342, LYON Cedex 07, France.*
[b] *Univ Lyon, INSA Lyon, Inria, CITI, EA3720, 69621 Villeurbanne, France*

Abstract

IEEE 802.11 has emerged as a vital wireless network access technology for mobile devices. By providing the potential for high connectivity speeds, this technology has led to a huge rise in the number of access points (APs). In such environments, mobile devices have the choice to join several Wi-Fi networks. Despite its importance to user Quality of Experience (QoE), the AP selection is still trivial since it focuses at best on the received signal strength if not only the user's history. Crucial metrics that capture the overall dynamics of the AP load condition, such as the network load, are not taken into account. In this paper, we propose to use the Busy Time Fraction (BTF) as a metric to choose the best AP to attach to. The BTF level of a given channel is inferred based on the frame aggregation scheme proposed since the 802.11n standard. In this regard, we build a proof of concept system, FAM (Frame Aggregation based method) that leverages the theoretical frame aggregation levels of a probe traffic returned by two analytical Markovian models and the measured ones in order to estimate not only the BTF but also the nature of the traffic. We validate the accuracy of our proposed approach against ns-3 simulations under several scenarios.

Keywords: IEEE 802.11 networks, aggregated MAC protocol data unit (A-MPDU), Performance evaluation, Network load, Markov chain

1. Introduction

As one of the cornerstones for delivering flexibility and high speeds, Wireless-Fidelity (Wi-Fi) or IEEE 802.11 has become the most used technology for accessing the Internet. Nearly, all companies, universities, and homes use Wi-Fi to satisfy their connectivity needs, which has led to the explosion of wireless data usage and the colossal rise of Access Points (APs), smartphones, and various mobile devices. According to [1], Internet users represented 3.9 billion in 2018,

*Corresponding author
Email addresses: nour-el-houda.bouzouita@ens-lyon.fr (Nour El Houda Bouzouita), anthony.busson@ens-lyon.fr (Anthony Busson), herve.rivano@inria.fr (Herve Rivano)

and they will exceed 5.3 billion by 2023, while the number of Wi-Fi hotspots will grow four-fold from 169 million hotspots in 2018 to nearly 628 million public Wi-Fi hotspots by 2023. With this huge proliferation, selecting the AP that offers the required performance is still a striking concern and a critical ongoing challenge.

In dense environments, a device seeking connectivity must choose among all the APs that are within its radio range. This association is initiated by the device's operating system based on the best Received Signal Strength Indicator (RSSI) or the user's history or preferences. RSSI or equivalent metrics may help to estimate the physical transmission rate that will be used. But, these simple criteria do not take into account the load of the channels, APs, or any information relative to the network performance imposed by the other stations and the current traffic.

On the one hand, aggressive Achievable throughput tests such as Ookla speedtest and iperf have widely been embraced for network performance measurements by typically measuring the TCP throughput. While throughput tests provide valuable insights into network state, they suffer from high intrusiveness (generated traffic) and dependence on transport and application protocol. Thus, making them a poor choice for performance characterization.

In contrast to these metrics, the network load seems to be an excellent fit since it conditions the throughput and gives a broader view of the network state independently of the transmission conditions of the device. This latter can be expressed in many ways. In this work, we consider the Busy Time Fraction (BTF), defined as the fraction of time the wireless medium is sensed busy due to successful or unsuccessful transmissions. It captures concurrent transmissions, constituting the AP load, as well as inter-network interference.

This paper aims at studying the possibility to infer the BTF of the channels used by the AP in its vicinity locally in the user space of a non-rooted vanilla device, typically a smartphone, without modifications on network equipment (STAs and APs). We consider an active probing approach (we send a probe traffic from a client to a server) to estimate this quantity between two devices connected to the same AP. A possible future application of this work (which is not considered in this paper) is to make these measurements available in a public database or through a crowd-sensing application in which participant mobile devices measure and share the load of their nearby networks. By building collective knowledge, other devices using the same application will be able to choose their AP as a function of the load and produce their own measures.

The classical channel load estimation tools based on time dispersion cannot be used in Wi-Fi [2, 3]. Indeed, in the most modern Wi-Fi versions (802.11n, ac, ax, and the most recent roll-up [4]), a frame aggregation scheme has been introduced. This scheme allows an AP or a station (STA) to send several frames through a unique access to the medium and thus making inter-packet arrival null. Hopefully, the load of the channel conditions the aggregation level, defined as the number of sub-frames within the same aggregated frame.

The contributions of our paper are as follows:

- We propose analytical models based on Markov chains that demonstrate how one could induce the theoretical frame aggregation levels of targeted probe traffic sent from a client to a server concurrent to the cross traffic (the competing traffic already present in the network).

- We reveal how the frame aggregation scheme embodies a rich set of Wi-Fi link properties that can be utilized to discern the network load. We illustrate through ns-3 simulations that frame aggregation levels correlate extremely well with the expected BTF across a variety of challenging scenarios. Moreover, we demonstrate that the throughput that a joining device could get depends on whether the competing traffic uses frame aggregation or not.

- We propose a method called Frame Aggregation based Method (FAM) that leverages both the theoretical frame aggregation levels (returned by the analytical models) and the measured ones to estimate not only the BTF but also the nature of the traffic (aggregated or not) which makes it possible to evaluate the available bandwidth that another device would have if it would join the network.

The proposed method constitutes a proof of concept that shows that the load is inferable locally when the server is close to the client, without any control on the AP. It is worth noting that it is not the definitive application and must potentially be supplemented by other methods depending on the context.

The paper is organized as follows. Section 2 describes in detail the background of this work. Section 3 presents our proposed analytical models to estimate the DownLink frame aggregation levels of the probe traffic and their validation. Section 4 exposes the proposed method. Section 5 is dedicated to the performance evaluation and numerical results of the method. Papers that relate to the studied problem are discussed in Section 6. We conclude this paper in Section 7.

2. Background

Before plunging into the details of our proposed system, we present several key background concepts. First, we give an overview of the IEEE 802.11 frame aggregation scheme in Section 2.1. We then give a brief description of how the AP queue handles packets under the frame aggregation.

2.1. Frame aggregation overview

Ever since their first introduction in 1997, IEEE 802.11 network has considerably enhanced its throughput by coming with new technological advances to improve the physical (PHY) and the Medium Access Control (MAC) layers. At the MAC layer, one of the significant steps forward was the introduction of the frame aggregation scheme by the IEEE 802.11n standard. Since then, this latter has become the default mechanism of sending data on modern Wi-Fi (802.11n,

ac, ax).

The general concept of frame aggregation is to allow several frames, that are destined to the same destination, to be clustered and sent out as one aggregated frame, and thus reducing the access time overhead (Distributed Inter Frame Space (DIFS), Back-off, etc.) and the PHY overhead as all the aggregated sub-frames share one PHY header. Frame aggregation can be achieved at two levels: at the Aggregate Mac Protocol Data Unit (A-MPDU) and the Aggregate MAC Service Data Unit. Since A-MSDU is rarely implemented, we focus on the A-MPDU aggregation.

Figure 1 depicts the structure of an aggregated frame. The A-MPDU aggregation consists in sending several sub-frames (A-MPDU) with a common Wi-Fi physical header (PHY Header). Each sub-frame is composed of an MPDU delimiter, followed by the MPDU, consisting of its own MAC header, MAC payload (a packet or any layer 3 Protocol Data Unit), and Frame Check Sequence (FCS). Padding bytes may be appended at the end.

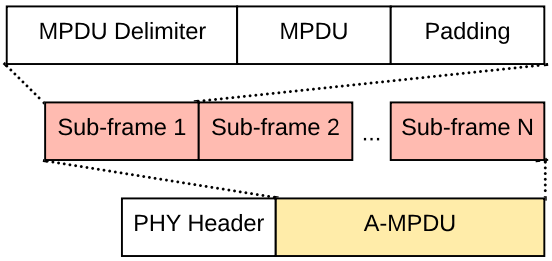

Figure 1: Illustration of A-MPDU frame aggregation.

2.2. AP queuing system under frame aggregation

Without frame aggregation and for a given enhanced distributed channel access (EDCA) class (an extension of the Distributed Coordination Function scheme that includes Quality of Service traffic prioritization for data packets), the AP pursues a predefined per-packet scheduling method (e.g., First In First Out (FIFO)). It is important to note that building a queuing algorithm is up to product designers that decide how to manage a transmission queue.

With frame aggregation, the aggregated transmissions act as a batch scheduler which alters the timing characteristics of received packets. To explain this approach, we show an example in Figure 2. It consists of an AP queue with two interleaved sequences of packets sent to two different clients, A and B, on a Wi-Fi link. Ai defines the i^{th} packet targeted to client A while Bi is the i^{th} packet destined to client B. In the case depicted in Figure 2, the packet at the head of the AP queue is addressed to A. All A's packets (within the limit of the maximum number of aggregated sub-frames) will be aggregated and sent out as an A-MPDU. Then, an aggregated frame with B's packets is sent. In this

paper, we consider this approach in order to build the first Markovian model (detailed in Section 3).

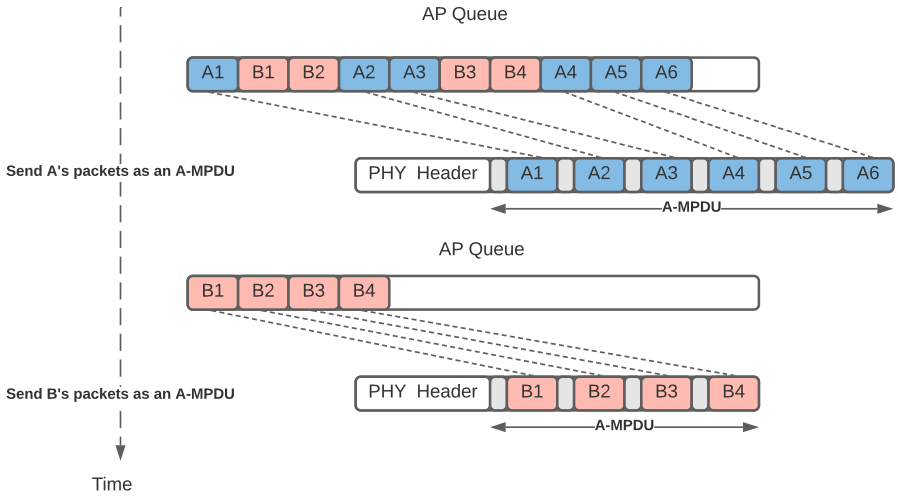

Figure 2: An Example of scheduling under frame aggregation.

3. Analytical models and their validation

In this section, we describe the proposed analytical models that help infer the frame aggregation behavior of the probe traffic as a function of the competing traffic. This competing traffic, called cross traffic, can aggregate its frames or not.

3.1. System model description

We now start by describing the system model coupled with a presentation of the common assumptions as well as the system notations used for the two analytical models.

We consider a general Wireless Local Area Network (WLAN) based on IEEE 802.11 Distributed Coordination Function (DCF) composed of two different entities: an AP and a user station. The station is assumed to be associated with the AP. Each station or AP has its own physical transmission rate. It is a combination of the following parameters: the modulation type and the coding rate which is defined by the Modulation and Coding Scheme index (MCS), the number of spatial streams, the channel width, and the guard interval length.

The two proposed analytical models are Discrete-Time Markov chains (DTMC). They appraise the frame aggregation levels of the DownLink probe traffic for a given cross traffic load in congested and non-congested networks. As the probe

frame aggregation levels depend on the nature of cross traffic (aggregated or non-aggregated traffic), the first chain considers that the cross traffic uses the frame aggregation scheme, whereas the second is based on non-aggregated cross traffic.

Table 1 summarizes the principal notations used in the models.

Table 1: Principal notations

Parameters (unit)	Definition
T_{DIFS} (μs)	Distributed Inter Frame Space duration
T_{SIFS} (μs)	Short Inter Frame Space duration
T_{PHY} (μs)	The preamble and PHY header duration
FCS ($Bytes$)	Frame Check Sequence
$T_{BlockACK}$ (μs)	Required time to send the block acknowledgment
$T_{backoff}$ (μs)	Average backoff time
T_{slot} (μs)	Slot time
CW_{min}	Minimum size of the contention window
Models notation	**Definition**
$P_{(i,j,k,u)(l,m,q,v)}$	Transition probability from state (i,j,k,u) to state (l,m,q,v)
T_{AP}(k) (μs)	Required time to send k DL probe aggregated packets
T_{SP}(k) (μs)	Required time to send k UL probe aggregated packets
$T_{AC}(K)$ (μs)	Required time to send k cross traffic sub-frames by the AP
T_{AC} (μs)	Required time to send a single cross traffic frame
d_c (μs)	Inter-arrival time of cross traffic sub-frames by the probe traffic node
d_p (μs)	Inter-arrival time of probe traffic sub-frames by the AP
$AMPDU_{AP}$	Maximum A-MPDU size for the AP
$AMPDU_P$	Maximum A-MPDU size for the probe traffic node

Our models rely on the following assumptions:

- **probe traffic:** we distinguish two types of probe traffics: 1) the UpLink (UL) probe traffic which is the traffic sent from the probe traffic node to the AP. It is a Constant Bit Rate (CBR) traffic, sent at regular interval d_p; and 2) the DownLink (DL) probe traffic forwarded to the probe server. Frame aggregation scheme is always enabled for this flow.

- **Cross traffic:** the cross traffic is modeled by a CBR source sending packets at regular interval d_c managed by a unique queue. The cross traffic can be either aggregated or not. This flow is coming from the distribution system (a wired network connected to the AP, which is not represented in Figures 3 and 5) and sent to the cross traffic node.

- **buffers:** the probe traffic node, the cross traffic node, and the AP buffers are assumed to have a finite size. More precisely, we assume that when an aggregated frame is sent for a given destination, the corresponding buffer

becomes empty for this destination. This assumption simplifies drastically the models and their computation. However, the simulation results show that it does not introduce a significant error.

The impact of these assumptions is evaluated through simulations and discussed in Section 3.2.

In building the two Markov chains, we first present the set of possible states and transitions and compute the transitions probabilities for each chain. We then detail the calculation of the stationary probabilities and the mean aggregation levels of the probe traffic for the two proposed models.

3.1.1. Model based on aggregated cross traffic

Figure 3 depicts the scenario considered in the model based on aggregated cross traffic. An AP and three stations operate on the same Wi-Fi channel. The AP is connected to a distribution system.

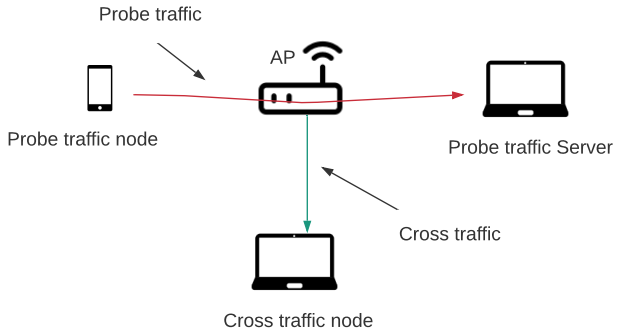

Figure 3: Scenario considered in the model based on aggregated cross traffic. The probe traffic node and server estimate the current load. The cross traffic aims to represent the current load of the system.

We now derive a mathematical model that estimates the frame aggregation levels of the DL probe traffic when we consider an aggregated cross traffic. This frame aggregation level is a function of the cross traffic. The model aims to be compared with the aggregation levels as measured by the probe traffic server to deduce the cross traffic load (load of the AP or channel).

The frame aggregation level of the DL probe traffic depends on the competition for medium access. In particular, when the cross traffic increases, the DL probe traffic has to wait longer. More packets may hence accumulate in the queue of the AP and be aggregated when the next DL probe transmission occurs.

We consider the Markov chain defined as $(X_n, Y_n, Z_n, S_n)_{n\geq 0}$. The process X_n describes the number of probe sub-frames contained in the AP queue at

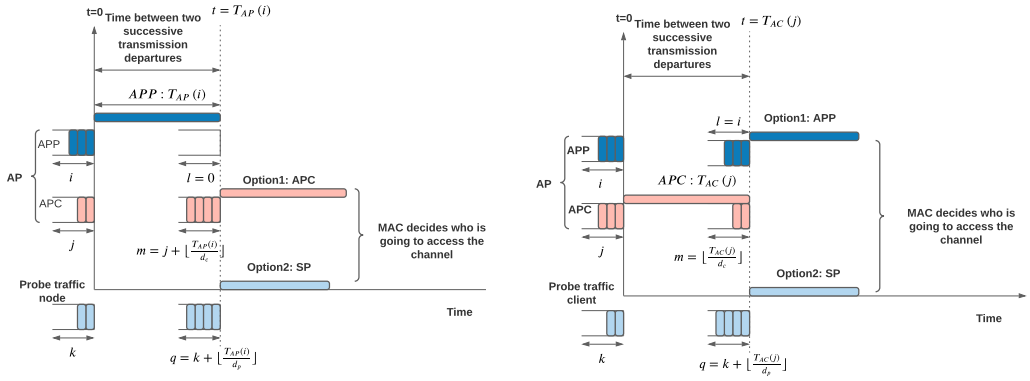

(a) Transition from APP

(b) Transition from APC

Figure 4: Possible transitions

the moment of the n^{th} frame transmission departure. The possible states are $\{0, .., AMPDU_{AP}\}$. Y_n defines the number of cross traffic sub-frames in the AP queue. The possible states are $\{0, .., AMPDU_{AP}\}$. The process Z_n represents the number of packets at the probe traffic client. The possible states are $\{0, .., AMPDU_P\}$. S_n describes the n^{th} transmission. It takes three possible values $\{APC,\ APP,\ SP\}$. APP (Access Point Probe) is a DL transmission of probe traffic from the AP. APC (Access Point Cross) denotes a cross traffic transmission from the AP to the cross server, while SP (Station Probe) corresponds to a UL transmission from the probe traffic client.

Transition probabilities. Having defined the set of possible states for each process, we shall now derive the transition probabilities. The transition probabilities are denoted $P_{(i,j,k,u)(l,m,q,v)}$, and represent the probability to go from state $(X_n, Y_n, Z_n, S_n) = (i, j, k, u)$ to state $(X_{n+1}, Y_{n+1}, Z_{n+1}, S_{n+1}) = (l, m, q, v)$.

The transition probabilities depend on the time between two successive transmissions. As both UL probe and UL cross traffics are deterministic, this time sets the number of packets that arrived in the AP buffer and the probing client buffer between two transmissions and thus the number of frames that will be sent in the next aggregated frame. We therefore analyze the events that may occur between two successive transmissions.

The next stage of our modeling is to decide when a transition from one state to another is allowed and to compute its probability. Note that impossible transitions have zero probability and that non-null transition probabilities are computed assuming that all concerned nodes are equally likely to access the channel. For ease of illustration, we categorize the state transitions into the following three classes.

Class I:Transition from state APP. For the sake of clarity, we recourse to Figure 4a to describe the possible transition probabilities and their computations. It illustrates an example of possible events between two successive transmissions when the current state is APP (an aggregated frame containing probe packets is transmitted by the AP). In this example, at time $t = 0$, we start from state (i, j, k, APP) (i.e (3,2,2,APP) in Figure 4a). The AP sends the i corresponding probe frames currently in its buffer ($i = 3$ in this example), aggregating them in a single A-MPDU using its current MCS. Its transmission duration is denoted $T_{AP}(i)$ which is given in Appendix A. Note that the AP has a single buffer that contains at once the probe and the cross traffics but in order to clarify the explanation of the model, we distinguish between them in Figure 4a.

During this transmission, the probe traffic node buffer receives $\lfloor \frac{T_{AP}(i)}{d_p} \rfloor$ packets and the AP buffer receives $\lfloor \frac{T_{AP}(i)}{d_c} \rfloor$ cross packets. As a result, at the end of the APP state, the probe traffic node buffer and the AP will contain respectively, $k + \lfloor \frac{T_{AP}(i)}{d_p} \rfloor$ of probe packets and $j + \lfloor \frac{T_{AP}(i)}{d_c} \rfloor$ of cross traffic packets ((4,4) in the Figure 4a).

At the end of this transmission, the buffer of the AP does not have probe frames to send ($X_{n+1} = 0$ almost surely), and another APP transmission is impossible ($S_{n+1} \neq APP$ almost surely). So from this state, only two transitions are allowed: to APC or SP with $X_{n+1} = l = 0$. It can occur only if $Y_{n+1} = m > 0$ and $Z_{n+1} = q > 0$ respectively.

We derive the non-null transition probabilities as follows. If the AP gains access to the channel, it will send the cross traffic currently in its buffer. For $m > 0$, the next transmission will be APC with probability:

$$P_{(i,j,k,APP)(l,m,q,APC)} = P\Big(S_{n+1} = APC | S_n = APP, X_{n+1} = l = 0, \\ Y_{n+1} = m > 0, Z_{n+1} = q\Big) \cdot \mathbb{1}_{k+\lfloor \frac{T_{AP}(i)}{d_p} \rfloor = q} \cdot \mathbb{1}_{j+\lfloor \frac{T_{AP}(i)}{d_c} \rfloor = m}$$

where $\mathbb{1}_{condition}$ is the indicator function that equals to 1 if *condition* is true and 0 otherwise. $P\Big(S_{n+1} = APC | S_n = APP, X_{n+1} = l = 0, Y_{n+1} = m > 0, Z_{n+1} = q\Big)$ denotes the probability that the event APC will occur given that the event APP has already occurred. In the interest of brevity, we postpone the computation of such probabilities to Appendix B.

Now, if the probe station gains access, the next event will be SP and the transition probability from APP to SP for $q > 0$ is given by:

$$P_{(i,j,k,APP)(l,m,q,SP)} = P\Big(S_{n+1} = SP | S_n = APP, X_{n+1} = l = 0, \\ Y_{n+1} = m, Z_{n+1} = q > 0\Big) \cdot \mathbb{1}_{k+\lfloor \frac{T_{AP}(i)}{d_p} \rfloor = q} \cdot \mathbb{1}_{j+\lfloor \frac{T_{AP}(i)}{d_c} \rfloor = m}$$

Class II:Transition from state APC. Once again, when presenting the transition probabilities of this class, we resort to Figure 4b. It depicts a timeline

of feasible events between two successive transmission departures when we start from the state APC.

The AP sends the j cross traffic frames currently in its buffer as an A-MPDU using the transmission rate associated to the cross traffic server. Its transmission duration is denoted $T_{AC}(j)$. During the period $T_{AC}(j)$, the probe traffic client buffer receives $\lfloor \frac{T_{AC}(j)}{d_p} \rfloor$ packets and the AP buffer receives $\lfloor \frac{T_{AC}(j)}{d_c} \rfloor$ cross traffic packets. At the end of the APC state, the probe traffic client buffer and the AP will thus contain respectively, $k + \lfloor \frac{T_{AC}(j)}{d_p} \rfloor$ of probe packets and $\lfloor \frac{T_{AC}(j)}{d_c} \rfloor$ of cross traffic packets.

Conversely to the previous class of transitions where only two possible transitions are allowed from the state APP, there are here three possible transitions under some conditions. S_{n+1} can be APP, APC, or SP.

First, we suppose that there will be another APC, the transition from APC to APC is deemed possible if and only if $X_n = i = 0$ and $Y_n = l = 0$: it is impossible to have two successive APC transmissions if $i > 0$ or $l > 0$ due to the AP queuing system detailed in Section 2.2. The transition probability from APC to APC with $Y_{n+1} = m > 0$ is:

$$P_{(0,j,k,APC)(0,m,q,APC)} = P\Big(S_{n+1} = APC | S_n = APC, X_n = X_{n+1} = 0, \\ Y_{n+1} = m > 0, Z_{n+1} = q\Big) \cdot \mathbb{1}_{\lfloor \frac{T_{AC}(j)}{d_c} \rfloor = m} \cdot \mathbb{1}_{k + \lfloor \frac{T_{AC}(j)}{d_p} \rfloor = q}$$

Now if we suppose that the AP gains the medium access to transmit the DL probe flow, the transition probability from APC to APP is possible only if $X_n = i = X_{n+1} = l$ since the AP cannot receive probe frames in its buffer during the transmission of the cross traffic and $X_{n+1} = l > 0$. The corresponding probability is given by:

$$P_{(i,j,k,APC)(l,m,q,APP)} = P\Big(S_{n+1} = APP | S_n = APC, X_{n+1} = X_n = l > 0, \\ Y_{n+1} = m, Z_{n+1} = q\Big) \cdot \mathbb{1}_{\lfloor \frac{T_{AC}(j)}{d_c} \rfloor = m} \cdot \mathbb{1}_{k + \lfloor \frac{T_{AC}(j)}{d_p} \rfloor = q}$$

If we assume that the probe traffic client gains the medium access, the transition from APC to SP is also allowed only if $X_{n+1} = l = X_n = i$ and $Z_{n+1} = q > 0$. We have:

$$P_{(i,j,k,APC)(l,m,q,SP)} = P\Big(S_{n+1} = SP | S_n = APC, X_{n+1} = X_n = l, \\ Y_{n+1} = m, Z_{n+1} = q > 0\Big) \cdot \mathbb{1}_{\lfloor \frac{T_{AC}(j)}{d_c} \rfloor = m} \cdot \mathbb{1}_{k + \lfloor \frac{T_{AC}(j)}{d_p} \rfloor = q}$$

Class III:Transition from state SP. In order to derive the transition probabilities of the last class, we apply the same principle. Due to space limitations, we do not describe the details of the derived transition probabilities.

From the SP state, there are three possible transitions APP, APC, or SP depending on the competition for the channel resource. First, if the next transition is APP with $X_{n+1} = l > 0$, the transition probability is given by:

$$P_{(i,j,k,SP)(l,m,q,APP)} = P\Big(S_{n+1} = APP | S_n = SP, X_{n+1} = l > 0, \\ Z_{n+1} = q, Y_{n+1} = m\Big) \cdot \mathbb{1}_{l=i+k} \cdot \mathbb{1}_{j+\lfloor \frac{T_{SP}(k)}{d_c} \rfloor = m} \cdot \mathbb{1}_{\lfloor \frac{T_{SP}(k)}{d_p} \rfloor = q}$$

Second, if the next transition is APC with $Y_{n+1} = m > 0$, the transition probability is defined as:

$$P_{(i,j,k,SP)(l,m,q,APC)} = P\Big(S_{n+1} = APC | S_n = SP, X_{n+1} = l, Y_{n+1} = m > 0, \\ Z_{n+1} = q\Big) \cdot \mathbb{1}_{l=i+k} \cdot \mathbb{1}_{j+\lfloor \frac{T_{SP}(k)}{d_c} \rfloor = m} \cdot \mathbb{1}_{\lfloor \frac{T_{SP}(k)}{d_p} \rfloor = q}$$

Finally, if the next transition is SP with $Z_{n+1} = q > 0$, the transition probability is thus formulated as:

$$P_{(i,j,k,SP)(l,m,q,SP)} = P\Big(S_{n+1} = SP | S_n = SP, X_{n+1} = l, Y_{n+1} = m, \\ Z_{n+1} = q > 0\Big) \cdot \mathbb{1}_{l=i+k} \cdot \mathbb{1}_{j+\lfloor \frac{T_{SP}(k)}{d_c} \rfloor = m} \cdot \mathbb{1}_{\lfloor \frac{T_{SP}(k)}{d_p} \rfloor = q}$$

3.1.2. Model based on aggregated cross traffic

Let us now derive the second Markov chain where the frame aggregation scheme is disabled for the cross traffic.

Figure 5 breaks down the network topology simulated by this model that consists of two co-located WLANs operating on the 2.4GHZ band. The first one enable the frame aggregation scheme (e.g., IEEE 802.11n in Figure 5) and the second one disable the frame aggregation (e.g., IEEE 802.11g in Figure 5). The 802.11n WLAN is composed of an AP and two nodes. A probe traffic node to send the UL probe traffic, and a server node to receive the forwarded DL traffic. The 802.11g WLAN is composed of an AP and a node that receives the non-aggregated cross traffic.

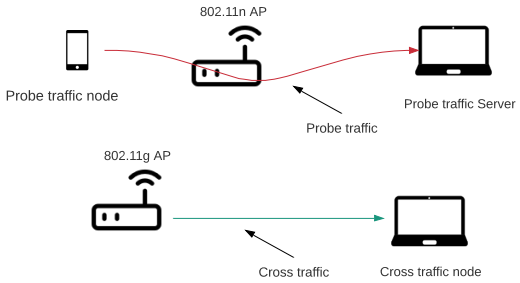

Figure 5: Scenario modeled by the model based on non-aggregated cross traffic.

The rationale behind this model is the same as the model described in the previous section except that each cross traffic transmission consists only of a single frame. Like the aggregated version of this model, we divide the state transitions into the following three classes for the non-aggregated version as follows.

Class I: Transition from APP. We first consider the transition probabilities when the current transmission is APP. Since during this transmission, the 802.11n AP sends an aggregated probe frame to the probe traffic server, the transitions probabilities from state APP are the same. We note that the computation of the conditional probabilities related to these three classes are given in Appendix C.

If the 802.11g AP gains access to the channel, the transition probability from state APP to state APC with $Y_{n+1} = m > 0$ is:

$$P_{(i,j,k,APP)(0,m,q,APC)} = P\Big(S_{n+1} = APC | S_n = APP, X_{n+1} = l = 0, \\ Y_{n+1} = m > 0, Z_{n+1} = q\Big) \cdot \mathbb{1}_{k+\lfloor \frac{T_{AP}(i)}{d_p} \rfloor = q} \cdot \mathbb{1}_{j+\lfloor \frac{T_{AP}(i)}{d_c} \rfloor = m}$$

Now if the probe traffic node gains the competition for the channel resource, the transition from APP to SP with $Z_{n+1} = q > 0$ is given by:

$$P_{(i,j,k,APP)(l,m,q,SP)} = P\Big(S_{n+1} = SP | S_n = APP, X_{n+1} = l = 0, \\ Y_{n+1} = m, Z_{n+1} = q > 0\Big) \cdot \mathbb{1}_{k+\lfloor \frac{T_{AP}(i)}{d_p} \rfloor = q} \cdot \mathbb{1}_{j+\lfloor \frac{T_{AP}(i)}{d_c} \rfloor = m}$$

3.1.3. Class II: Transition from APC

We second consider the transition probabilities when the current transmission is APC. When presenting the probabilities of this class, we resort to Figure 6. It exposes a set of possible events between two successive transmission departures when we start from the state APC.

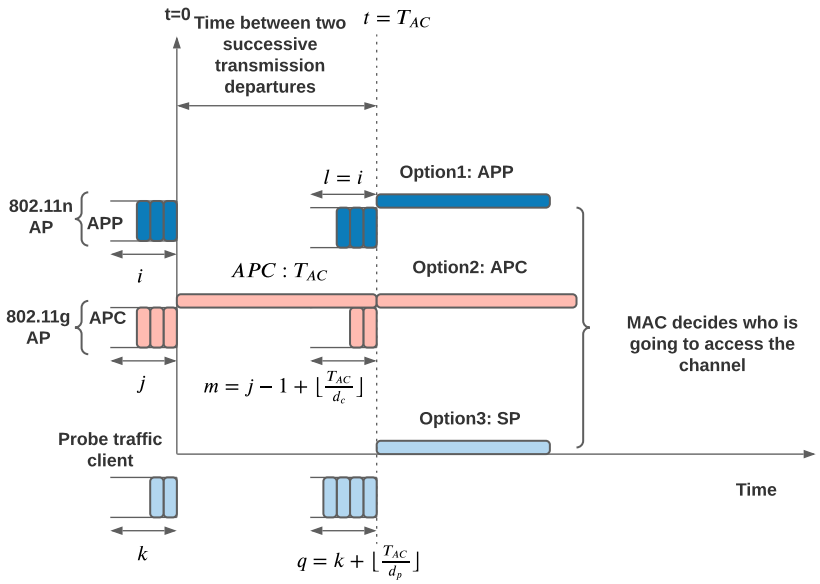

Figure 6: Possible events between two successive transmissions for the *Wireless server* model based on non-aggregated cross traffic when the current transmission is APC.

The 802.11g AP sends a single frame from the j cross traffic frames currently in its buffer. Its transmission duration is denoted T_{AC}. During this period, the probe traffic node receives $\lfloor \frac{T_{AC}}{d_p} \rfloor$ of probe packets, and the 802.11g AP receives $\lfloor \frac{T_{AC}}{d_c} \rfloor$ of cross traffic.

Here, there are three possible transitions. The process S_{n+1} can be APP, APC, or SP. It should be noted that all the following transitions are deemed possible if $X_n = i = X_{n+1} = l$ since the 802.11n AP cannot receive probe frames in its buffer during the transmission of the cross traffic by the 802.11g AP.

If we assume that there will be another APC, the corresponding probability with $Y_{n+1} = m > 0$ is defined as follows:

$$P_{(i,j,k,APC)(l,m,q,APC)} = P\Big(S_{n+1} = APC | S_n = APC, X_{n+1} = X_n = i = l, \\ Y_{n+1} = m > 0, Z_{n+1} = q\Big) \cdot \mathbb{1}_{j-1+\lfloor \frac{T_{AC}}{d_c} \rfloor = m} \cdot \mathbb{1}_{k+\lfloor \frac{T_{AC}}{d_p} \rfloor = q}$$

Now if we expect that there will be APP, the transition probability from APC to APP with $X_{n+1} = l > 0$ is given by:

$$P_{(i,j,k,APC)(l,m,q,APP)} = P\Big(S_{n+1} = APP | S_n = APC, X_{n+1} = X_n = i = l \\ = l > 0, Y_{n+1} = m, Z_{n+1} = q\Big) \cdot \mathbb{1}_{j-1+\lfloor \frac{T_{AC}}{d_c} \rfloor = m} \cdot \mathbb{1}_{k+\lfloor \frac{T_{AC}}{d_p} \rfloor = q}$$

Finally, we establish the transition probabilities from APC to SP. This transition is allowed if $Z_{n+1} = q > 0$ and given by:

$$P_{(i,j,k,APC)(l,m,q,SP)} = P\Big(S_{n+1} = SP | S_n = APC, X_{n+1} = X_n = i = l, \\ Y_{n+1} = m, Z_{n+1} = q > 0\Big) \cdot \mathbb{1}_{j-1+\lfloor \frac{T_{AC}}{d_c} \rfloor = m} \cdot \mathbb{1}_{k+\lfloor \frac{T_{AC}}{d_p} \rfloor = q}$$

3.1.4. Class III: Transition from SP

We now derive the transition probabilities of the last class of this model. From the state SP, there are also three possible transitions APP, APC, or SP depending on the competition for the channel resource.

First, if the next transition is APP with $X_{n+1} = l > 0$, the transition probability is given by:

$$P_{(i,j,k,SP)(l,m,q,APP)} = P\Big(S_{n+1} = APP | S_n = SP, X_{n+1} = l > 0, \\ Y_{n+1} = m, Z_{n+1} = q\Big) \cdot \mathbb{1}_{l=i+k} \cdot \mathbb{1}_{j+\lfloor \frac{T_{SP}(k)}{d_c} \rfloor = m} \cdot \mathbb{1}_{\lfloor \frac{T_{SP}(k)}{d_p} \rfloor = q}$$

Second, if the next transition is APC with $Y_{n+1} = m > 0$, the transition probability is formulated as:

$$P_{(i,j,k,SP)(l,m,q,APC)} = P\Big(S_{n+1} = APC | S_n = SP, X_{n+1} = l, Y_{n+1} = m > 0 \\ Z_{n+1} = q\Big) \cdot \mathbb{1}_{l=i+k} \cdot \mathbb{1}_{j+\lfloor \frac{T_{SP}(k)}{d_c} \rfloor = m} \cdot \mathbb{1}_{\lfloor \frac{T_{SP}(k)}{d_p} \rfloor = q}$$

Finally, if the next transition is SP with $Z_{n+1} = q > 0$, the transition probability is thus formulated as:

$$P_{(i,j,k,SP)(l,m,q,SP)} = P\Big(S_{n+1} = SP | S_n = SP, X_{n+1} = l, Y_{n+1} = m, \\ Z_{n+1} = q > 0\Big) \cdot \mathbb{1}_{l=i+k} \cdot \mathbb{1}_{j+\lfloor \frac{T_{SP}(k)}{d_c} \rfloor = m} \cdot \mathbb{1}_{\lfloor \frac{T_{SP}(k)}{d_p} \rfloor = q}$$

3.1.5. Stationary probability

So far, we have evaluated all the transition probabilities. The last phase consists in deriving the stationary probability and computing the frame aggregation levels. Let us remind that a Markov chain is irreducible if and only if every state can be reached by any other state through one or several transitions. As our Markov chain is irreducible and has a finite number of states, hence it exists a unique stationary distribution. We solve this Markov chain through a numerical method. We compute the stationary probabilities and we denote by π the vector containing the corresponding values. The mean DL probe traffic aggregation levels, denoted $MeanAgg$ are then given by: $MeanAgg = \sum_{n=1}^{AMPDU_{AP}} n \cdot \pi_n$.

3.2. Numerical results

In this section, we evaluate the accuracy of the proposed models in estimating the frame aggregation levels of the probe traffic. We do so under several scenarios with different network parameters, such as the topology and its size, different IEEE 802.11 amendments, and different traffic patterns. In this regard, we compare the aggregation levels given by the models with those delivered by the discrete-event network simulator 3 (ns-3 version 3.30). For simplicity reasons, we assume for all the scenarios that all nodes have a random but fixed position during the whole simulation duration. We compute the two models for six cross traffic loads/BTF levels: 0, 0.125, 0.25, 0.375, 0.5, and 0.625 ranging from low to high levels of BTF. The maximum numbers of aggregated sub-frames $AMPDU_P$ and $AMPDU_{AP}$ are set to 36.

3.2.1. Validation of the model based on aggregated cross traffic

We now examine the accuracy of the first model where the frame aggregation scheme is enabled for both probe and cross traffics under the 802.11n standard amendment.

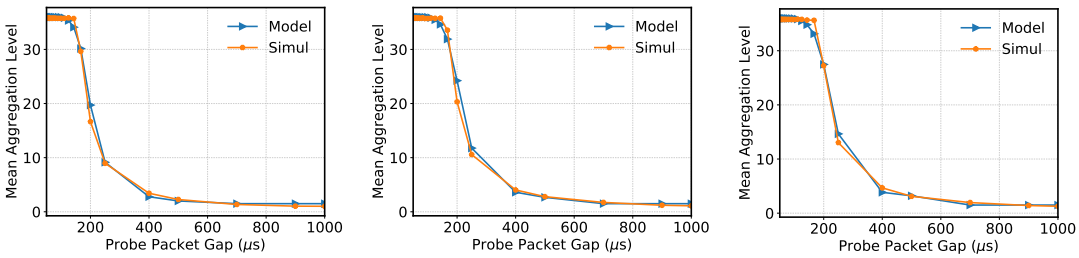

(a) BTF=0.25. (b) BTF=0.375. (c) BTF=0.5.

Figure 7: Mean aggregation levels of the model based on aggregated cross traffic versus ns-3 simulations - Same MCS.

Scenario #1 - Same MCS. We start by examining the performance details of this model when the same MCS index (HT-MCS15 with a physical transmission rate of 144.4 Mbps) is used for the probe traffic node and the AP. Figure 7 shows the mean aggregation level for the probe traffic as a function of the probe packet gap for the model and simulations. We let the probe packet gap gradually varies from 50μs to 1000μs. According to these results, it appears that the model performs well since it follows closely the pattern of the ns-3 simulations for the three levels of the network loads (0.25, 0.375, and 0.5). It is also the case for the three other BTFs (0, 0.125, and 0.625) that are not shown here. We can observe that the aggregation levels depend on the loads of the network. Indeed, when the BTF increases, the probe traffic has to wait longer, and more packets are received between two successive probe transmissions.

Scenario #2 - Different MCS indexes. We now evaluate the performance details of the first model when different MCS indexes are used for the probe traffic node and the AP.

Figure 8 shows the corresponding results. Figure 8a plots the results when we use the MCS 15 (144.4 Mbps) for the AP to send the DL probe traffic and the cross traffic and the MCS11 (57.8 Mbps) for the probing node. Figure 8b provides the corresponding results when we use MCS15 for the AP and MCS13 (115.6 Mbps) for the probe traffic node. The results show that considering different MCS indexes for the AP and the probe traffic node does not impact the accuracy of our approach.

Scenario #3 - Exponential On/Off cross traffic. To provide a broader overview of the accuracy reached by the proposed modeling approach, this scenario simulates another traffic pattern for the cross traffic which is exponential On/Off traffic, reflecting some of the kinds of cross traffic that would occur in practice. In ns-3, we use exponentially distributed On/Off periods thanks to the ns-3 OnOff Application class. This latter mainly relies on an *OffTime* and *OnTime* duration attributes that represent respectively the duration during which the data transfer is switched off and the duration of the continuous data transfer.

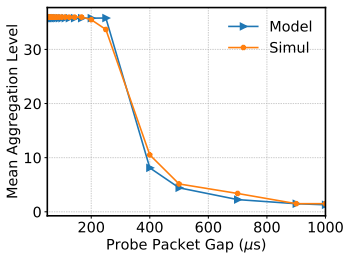

(a) BTF= 0.375, MCS 11 for the probe traffic node.

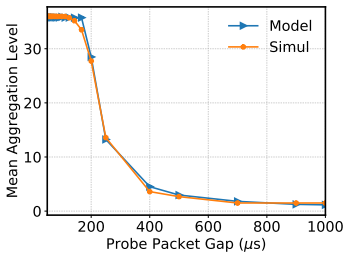

(b) BTF= 0.375, MCS 13 for the probe traffic node.

Figure 8: Mean aggregation levels of the model based on aggregated cross traffic versus ns-3 simulations - Different MCS indexes.

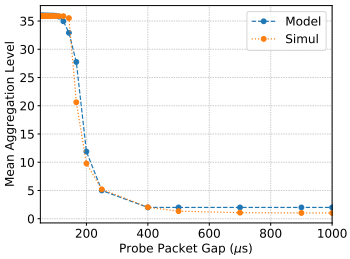

(a) BTF=0.125

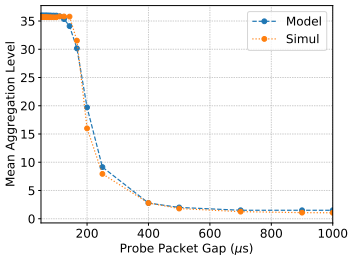

(b) BTF=0.25.

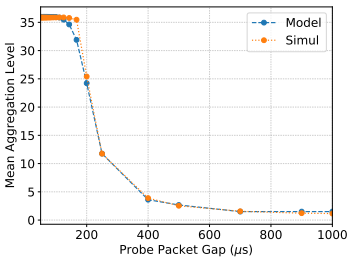

(c) BTF=0.375.

Figure 9: Mean aggregation levels of the model based on aggregated cross traffic versus ns-3 simulations - Exponential On/Off cross traffic.

Figure 9 shows the mean aggregation levels for the BTFs 0.125, 0.25 and 0.375. These results show that the estimations made by our model fit those delivered by ns-3 for the exponential On/Off aggregated cross traffic. We conclude that the proposed models still perform well under exponential On/Off traffic pattern.

Scenario #4 - 802.11ax traffic. Here, we run the first model when both the probe and cross traffics use the 802.11ax standard. All the nodes use the data rate=286.8Mbps. It is noticeable from Figure 10 that the mean aggregation levels obtained with simulations fit the ones from the model.

3.3. Validation of the model based on non-aggregated cross traffic

We now examine the accuracy of the model based on non-aggregated cross traffic under several scenarios.

Scenario #1 - Three STAs. We consider the same scenario described in Figure 5. We compare the aggregation levels given by this model to the ns3 simulations' outcomes. The results are plotted in Figure 11 for the three levels of BTF: 0.375, 0.5 and 0.625.

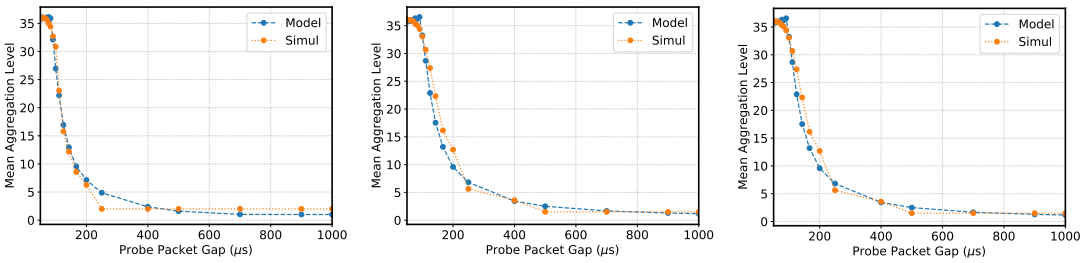

(a) BTF=0.125. (b) BTF=0.375. (c) BTF=0.5.

Figure 10: Mean aggregation levels of the model based on aggregated cross traffic versus ns-3 simulations - 802.11ax traffic.

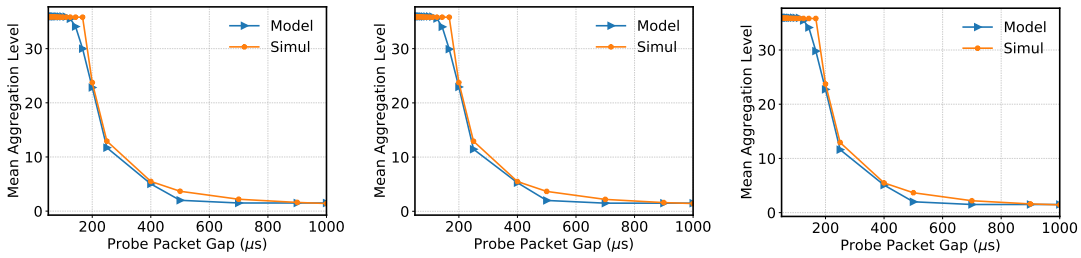

(a) BTF=0.375. (b) BTF=0.5. (c) BTF=0.625.

Figure 11: Mean aggregation levels of the model based on non-aggregated cross traffic versus ns-3 simulations - Three STAs.

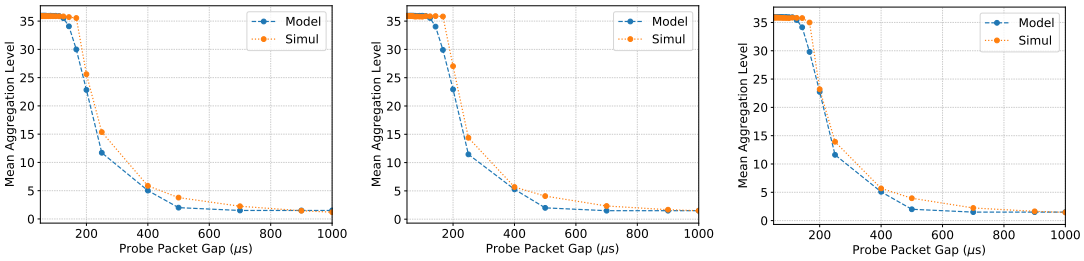

(a) BTF=0.375. (b) BTF=0.5. (c) BTF=0.625.

Figure 12: Mean aggregation levels of the model based on non-aggregated cross traffic versus ns-3 simulations - Six STAs.

Based on this figure, we observe that the model is able to reproduce the DL probe traffic aggregation behavior for the three BTFs with a satisfying degree of precision.

Scenario #2 - Six STAs. We now consider the case where we increase the number of competing cross traffic nodes from one to four. The results shown in Figure 12 reveal that the number of stations composing the DL competing traffic coming from the same AP does not influence the estimations for the model.

Overall, these analytical solutions are found to be accurate delivering estimates in good agreement with the simulations results for the considered scenarios.

Figures 13b and 13a show the probe mean aggregation levels for each of the six BTFs when the frame aggregation scheme is disabled or enabled for the cross traffic respectively. Based on Figure 13b, we can see that varying the level of cross traffic barely affects the probe aggregation levels when the $BTF > 0.25$. In this case, each cross traffic frame is sent independently, with short transmission times. Consequently, the probe traffic receives less packets to aggregate between two consecutive medium accesses. Also, cross traffic reaches saturation faster (as it sends less frames on average). As soon as it has always a frame to send, its access time does not depend on its buffer state. Consequently, the aggregation level of the probe traffic becomes insensitive to the level of congestion of the cross traffic. On the contrary (Figure 13a), when cross traffic aggregates its frames, the state of its buffer has a deeper impact on probe traffic aggregation since the cross traffic buffer state determines the transmission duration. These results nicely highlight the fact that varying the level of the aggregated network load significantly affects the probe aggregation levels. Consequently, the results are sufficiently separated to be used to infer the load level (Section 4).

4. Description of the method FAM

The previous section proposed Markovian analytical models to estimate the theoretical aggregation levels of the probe traffic and compiled a series of ob-

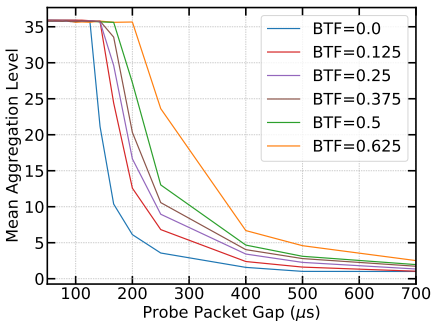

(a) Simulated Mean Aggregation levels for all BTFs when the cross traffic does not aggregates its frames.

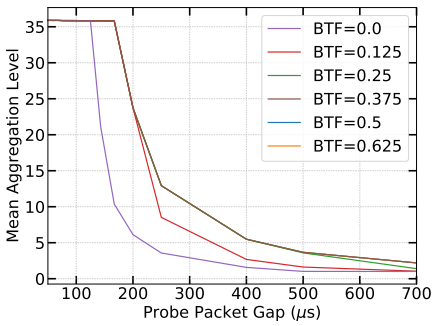

(b) Simulated Mean Aggregation levels for all BTFs when the cross traffic aggregates its frames.

Figure 13: Mean aggregation levels versus BTFs, cross traffic aggregates or not its traffic.

servations indicating that we can rely on this estimation to infer the network load for modern Wi-Fi networks. Specifically, we find a strong correlation between the aggregation levels of the probe traffic and the network load. This realization actually gives a stepping stone to designing a system able to infer the latter from the former. In this section, we hence introduce a network load inference method called Frame Aggregation based Method (FAM). It exploits the rich information embedded in frame aggregation to infer both the BTF of an AP and the type of traffic. Note that no changes are required, neither to the device nor to the AP. The designed system aims at achieving this estimation for unmodified mobile devices.

The foundation of FAM is mainly built on three steps:

- Measurement of the mean aggregation levels for different traffic flows. (Section 4.1)
- Detection of the type of the cross traffic (Section 4.2)
- Estimation of the wireless channel load (Section 4.3)

We unfold the details of the proposed approach by exposing the algorithmic representation of each stride. Each step relies on one or many algorithms. We note that all the algorithms detailed below are implemented on the server except the client procedure (Algorithm 1), which is implemented on the robe traffic node. (as shown in Figure 14).

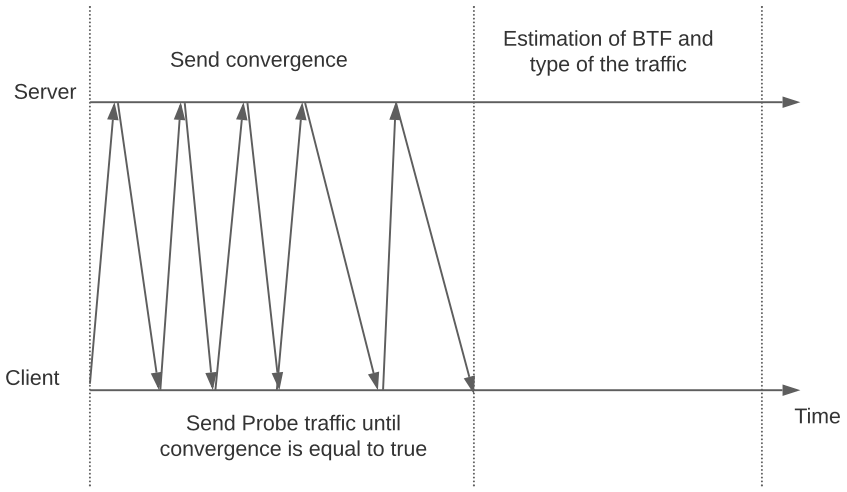

Figure 14: FAM work flow.

4.1. Mean aggregation level

Initially, we start with the measurement of the aggregation levels of the probe traffic. This process is described in algorithms 1 and 2. Algorithm 1 runs on the probing node. It begins by sending successive batches of probe packets. For each batch, the gap interval between packets, d_p, is increased from $d_{p_{min}}$ to $d_{p_{max}}$. In order to evaluate the mean aggregation levels accurately while keeping the batch size as small a possible, the number of packets in a batch np is not fixed. This number is determined using the Central Limit Theorem (CLT) detailed in the server procedure (Algorithm 2). Upon receipt of this batch, the server responds with a packet that indicates to the probe node to stop sending packets. It is the *convergence* variable in the algorithm.

Algorithm 1 Client Procedure

Input: K_{max} : Maximum A-MPDU Length, np : size of a batch of probes

$d_{p_{min}} = \frac{f(K_{max})}{K_{max}}$
$d_p = d_{p_{min}}$
repeat
  repeat
    client.send (d_p, np) ▷ Send np packets with interval d_p
    client.receive(convergence)
  until convergence is True
  client.receive($meanAgg$)
  $d_p = d_p$+increment
until $meanAgg > 2$
client.send(0, 1) ▷ Send 1 packet to inform that the campaign is finished.

Algorithm 2 Server Procedure

Input: E :acceptable standard error of the mean, Z : Value of the distribution function

MeanAgg=$\emptyset$, D=$\emptyset$
while campaign in progress for this client **do**
  $n = 0$, convergence = False, $meanAgg = 0$
  while !convergence **do**
    server.receive(1) ▷ Reception of the first packet that contains the parameters (d_p, np)
    server.receive($np - 1$) and store $agg_{i+n},\ \forall i \in \{1, np\}$
    $n = n + np$
    $meanAgg = \frac{\sum_{j=1}^{n} agg_j}{n}$
    $S^2 = \frac{1}{n-1} \sum_{i=1}^{n} (agg_i - meanAgg)^2$
    $convergence = \left(n \geq \frac{Z^2 \times S^2}{E^2}\right)$
    server.send(convergence)
  end while
  Add $meanAgg$ to vector MeanAgg
  Add d_p to vector D
  server.send($meanAgg$)
end while

Output: (MeanAgg, D) ▷ Returns two vectors: the "MeanAgg" and "D"

On the other side, Algorithm 2 runs on the server. It receives and processes the incoming probe packets from the probe traffic node. During a given batch, the mean aggregation is computed on the fly at the reception of probe packets. We use the CLT to evaluate the accuracy of the mean aggregation levels. When the error is lower than the expected error E, the server sends the *convergence* notification to the probe node (that stops its batch). The use of the CLT allows the application to appropriately measure the mean aggregation level with a minimal amount of time and bandwidth cost.

4.2. Cross traffic nature

Having already computed the mean aggregation levels of the probe traffic, we now proceed with the cross traffic type estimation. Our intuition and reasoning to assess the cross traffic nature is based on the idea that, if the cross traffic does not aggregate, its channel access time becomes constant when the channel load increases. This time is defined here as the time the cross traffic uses the channel between two successive probe traffic accesses. It corresponds to $T_{AC} + T_{AC}$ in Figure 6. The cross traffic access time depends only on the successive number of times it accesses the channel and the time to transmit a single frame. When the two buffers (cross and probe) are non-empty, it becomes independent of the number of frames/packets in these buffers and thus on the probe and traffic loads. On the contrary, when the cross traffic aggregates its frames, this time is increasing with the load as A-MPDU contains more aggregated frames.

We use this observation to detect the nature of the cross traffic. The mean cross traffic access time is denoted T_C. If this time is constant with d_p and with the load, we can express the mean aggregation level for the probe traffic, *meanAgg*, through a fixed point equation.

$$meanAgg = min\left(K_{max}, \frac{f(meanAgg)}{d_p} + \frac{T_C}{d_p}\right) \quad (1)$$

The rational of this equation is that the mean number of aggregated frames (*meanAgg* on the left-hand side of the equation) is equal to the number of frames received at the buffer since the last probe transmission. In Figure 6, we would get $X_{n+1} = \frac{T_{AP}(X_n)}{d_p} + \frac{T_{AC}+T_{AC}}{d_p}$. Substituting (X_n, X_{n+1}) by the mean aggregation ($X_n = X_{n+1} = meanAgg$) and assuming that the cross traffic access time is constant, $(T_{AC} + T_{AC})$ becomes T_C for this example), we obtain the Equation 1.

This approach is described in Algorithm 3. It takes as input the mean aggregation level for the probe and computes T_C, according to equation 1, for each probe packet gap d_p. It keeps only values of T_C for which $\frac{T_{AP}(meanAgg)}{d_p} + \frac{T_C}{d_p}$ is less than K_{max}. Then, it returns the percentage of variation between the maximum and minimum of these values. In Algorithm 6, this percentage is compared to a given threshold to determine if T_C can be considered as constant (cross traffic does not aggregate) or not (cross traffic aggregates).

Algorithm 3 Percentage Increase Algorithm

Input: MeanAgg=$(meanAgg(d_{p_{min}}), ..., meanAgg(d_{p_{max}}))$,
D=$(d_{p_{min}}, ..., d_{p_{max}})$
1: $TC\_VECTOR = \emptyset$
2: **for** all $d_p \in D$ **do**
3: Compute T_C:
4: $T_C(d_p) = d_p * meanAgg(d_p) - f(meanAgg(d_p))$
5: **if** $\frac{f(meanAgg)}{d_p} + \frac{T_C}{d_p} < K_{max}$ **then**
6: Add $T_C(d_p)$ to vector TC_VECTOR
7: **end if**
8: **end for**
9: $\%increase \leftarrow \frac{max(TC\_VECTOR)-min(TC\_VECTOR)}{min(TC\_VECTOR)} * 100$
Output: $\%increase$

4.3. BTF estimation

Having already computed the mean aggregation levels and discussed how to determine the type of the concurrent traffic, we now detail how to estimate the network of a wireless channel via its BTF.

Two algorithms are proposed to estimate the BTF. They are both based on the comparison between the mean aggregation levels given by our Markov chains and the measures made for different probe traffic batches.

Algorithm 4 BTF Error Based Method Algorithm

Input: MeanAgg=$(meanAgg(d_{p_{min}}), ..., meanAgg(d_{p_{max}}))$,
D=$(d_{p_{min}}, ..., d_{p_{max}})$
1: **for each** $case \in \{w/A, wo/A\}$ **do**
2: **for** $bt \in$ levels of BTF **do**

$$Error_{(bt,case)} = \frac{1}{Size(MeanAgg(.))} \sum_{d_p=d_{p_{min}}}^{d_{p_{max}}} \mid model_{(case,d_p,bt)} - meanAgg(d_p) \mid$$

3: **end for**
Output: $(\text{argmin}_{bt}\, Error_{(bt,w/A)}, \text{argmin}_{bt}\, Error_{(bt,wo/A)})$
4: **end for**

Algorithm 4 computes the mean error as the sum of the difference between the model and the measures. It returns the BTF that minimizes this error. The considered levels of BTF are a parameter of the algorithm. It returns a BTF for the model with aggregation (w/A) and a BTF for the model without frame aggregation (wo/A).

Algorithm 5 considers a notion of score to infer the BTF. For each probe packet gap d_p and a given model, the BTF that minimizes the error scores one. For each model, the final BTF will be the one that maximizes this score.

Algorithm 5 BTF Score Based Method Algorithm

Input: MeanAgg=$(meanAgg(d_{p_{min}}), ..., meanAgg(d_{p_{max}}))$,
D=$(d_{p_{min}}, ..., d_{p_{max}})$
1: **for** $d_p \in D$ **do**
2: **for each** $case \in \{w/A, wo/A\}$ **do**
3: **for** $bt \in$ all levels of BTF **do**
4: $Error(case, d_p, bt) = \frac{1}{Size(meanAgg(.))} \mid model(case, d_p, bt) - meanAgg(d_p) \mid$
5: **end for**
6: **end for**
7: $Score(\text{argmin}_{bt,case}\, Error(case, d_p, bt), case) += 1$
8: **end for**
Output: $(\text{argmax}_{bt}\, Score(bt, w/A), \text{argmax}_{bt}\, Score(bt, wo/A))$

Algorithm 6 gives the final output of our method. First, it evaluates if the BTF is less or equals to 0.25. We have observed that, for such a low load, it is difficult to distinguish precisely the nature of the traffic since the cross traffic tends to have very small mean aggregation levels. In this case, no precision on the aggregation is given. If the BTF is greater than 0.25 at least for one of the two models, it computes the percentage of variation of T_C with Algorithm 3 and compares it to a threshold T. It determines if the cross traffic access time

can be considered as constant and consequently if the cross traffic aggregates or not. For both cases, the corresponding BTF is returned with the cross traffic nature.

Algorithm 6 BTF Estimation Algorithm

Input: T:Threshold, E: acceptable standard error of the mean

(MeanAgg, D) = Server Procedure(E, Z)
$PI = PercentageIncrease(MeanAgg, D)$
$BTF_{w/A}, BTF_{wo/A}$ = Error Computation Procedure(MeanAgg,D)
$BTF1_{w/A}, BTF1_{wo/A}$ = Score Computation Procedure(MeanAgg,D)
if ($BTF_{w/A} \leq 0.25$ *or* $BTF1_{w/A} \leq 0.25$) *and* ($BTF_{wo/A} \leq 0.25$ *or* $BTF1_{wo/A} \leq 0.25$) **then**
    return $\{wo/A, BTF \leq 0.25\}$
else if $0 < PI < T$ **then**
    return $\{wo/A, BTF > 0.25\}$
else
    return $\{w/A, BTF_{w/A}\}$
end if

As a summary, in this section, we introduced the algorithmic details of the system FAM. We start by installing a dedicated client application on the probe traffic node, that sends a probing flow to the server. This latter uses the packet reception time to estimate the mean aggregation levels that, in turn, will serve to discern the BTF and convey the network nature.

5. Performance Evaluation

In this section, we evaluate the accuracy of the proposed method FAM by relying mainly upon the same ns-3 scenarios used in the Section 3 that expose different network parameters, different IEEE 802.11 amendments, and different traffic patterns.

The parameters of our method are as follow. Similar to the analytical models, we compute the four Markovian models for six cross traffic loads/BTF levels: 0, 0.125, 0.25, 0.375, 0.5, and 0.625 ranging from low to high levels of BTF. In algorithm 2, the FAM method uses a 95% confidence interval ($Z = 1.96$) and an error $E = 0.05$. The CLT results indicated that the relevant number of packets to send increases proportionally to the probe rate. The number of sent packets ranges between 600 and 3800. In algorithm 6, the threshold T is chosen according to an empirical method. Our simulations and experiments have shown that a value of $T = 200\%$ offers good performances. For instance, we take different values for the parameter T that depend on the device's transmission rate. These values are known by FAM.

5.1. FAM validation for aggregated cross traffic scenarios

In this section, we assess the effectiveness of FAM when relying on the theoretical aggregation levels returned by the models when the cross traffic uses

or not the frame aggregation feature. We want to evaluate the ability of FAM to infer the BTF and the cross traffic type when we consider aggregated cross traffic scenarios.

Scenario #1 - Same MCS. We now study the case when all the nodes (AP and STAs) use the same MCS index (MCS15 corresponding to 144.4 Mbps). We reuse the three-STAs scenario of Figure 3.

Results presented in table 2 show that the method finds the good results for all the levels of BTF.

Table 2: BTF and cross traffic nature estimations for ns3 simulations where the cross traffic is aggregated - Same MCS

Ground Truth BTF	Estimated BTF and cross traffic nature					
	Cross traffic aggregates				Cross traffic does not aggregate	
	≤ 0.25	0.375	0.5	0.625	≤ 0.25	> 0.25
0	S/A				S/A	
0.125	S/A				S/A	
0.25	S/A				S/A	
0.375		S/A				
0.5			S/A			
0.625				S/A		

Scenario #2 - Different MCS indexes. Once again, we consider the scenario depicted in Figure 3 to study the accuracy of our approach under nodes (AP and STAs) that have different data rates. We use the MCS15 (144.4 Mbps) for the AP to send the DL probe traffic and the cross traffic and the MCS11 (57.8 Mbps) for the probing node (scenario 1). Then, we use MCS15 for the AP and MCS13 (115.6 Mbps) for the probe traffic node (scenario 2).

Table 3 shows the results of scenario 2. We can observe that the method finds the good results for the five BTFs 0, 0.25, 0.375, 0.5, and 0.625 and slightly overestimates the BTF for the case 0.125. This error is only of 0.125 (approximately 10%) and is due to the fact that we neglect some protocol aspects, such as the beacons sent by the AP. We note that we obtain similar results as 3 for the scenario 2.

Overall, we notice that despite having STAs with significantly different data rates, the method FAM is still able to deliver reasonable predictions for the BTF.

Table 3: BTF and cross traffic nature estimations for ns3 simulations where the cross traffic is aggregated - Different MCS

Ground Truth BTF	Estimated BTF and cross traffic nature					
	Cross traffic aggregates				Cross traffic does not aggregate	
	≤ 0.25	0.375	0.5	0.625	≤ 0.25	> 0.25
0	S/A				S/A	
0.125	S	A			S	
0.25	S/A				S/A	
0.375		S/A				
0.5			S/A			
0.625				S/A		

Scenario #3 - Exponential On/Off cross traffic. Instead of taking into account deterministic cross traffic, this scenario considers cross traffic generated using exponentially distributed On/Off periods.

Table 4 shows the results returned by FAM for the corresponding scenario. It can be seen that FAM predicts reasonably well the BTF values and the cross traffic nature for the 0, 0.125, 0.25, 0.375 and 0.625 cases and slightly overestimates the BTF for the 0.5 case.

Overall, despite a slight discrepancy in estimating the precise level of BTF in some cases, the results returned by the method are in good agreement with those provided by the simulations.

Table 4: BTF and cross traffic nature estimations for ns3 simulations - Exponential On/Off aggregated cross traffic

Ground Truth BTF	Estimated BTF and cross traffic nature					
	Cross traffic aggregates				Cross traffic does not aggregate	
	≤ 0.25	0.375	0.5	0.625	≤ 0.25	> 0.25
0	S/A				S/A	
0.125	S/A				S/A	
0.25	S/A				S/A	
0.375		S/A				
0.5			S	A		
0.625				S/A		

Scenario #4 - 802.11ax traffic. In order to further assess the validity of the approach, in this scenario, we study FAM's accuracy when relying on 802.11ax aggregated probe and cross traffics in the 2.4 GHz band. All the nodes (AP and stations) operate at HE-MCS11 corresponding to $286.8 Mbps$. The network topology is the same as the scenario depicted in Figure 3. We run our FAM

method while considering an empirical threshold T equal to 100.

The results of FAM are shown in table 5. It can be seen that FAM predicts reasonably well the BTF values for all the cases except the fifth case: BTF=0.5 with 10% of error. In addition, it predicts well the nature of the traffic for all the cases. We, therefore, can conclude that FAM provides results that match well with the simulations under 802.11ax when relying on theoretical estimates provided by the models.

Table 5: BTF and cross traffic nature estimations for ns3 simulations - 802.11ax traffic

Ground Truth BTF	Estimated BTF and cross traffic nature					
	Cross traffic aggregates				Cross traffic does not aggregate	
	≤ 0.25	0.375	0.5	0.625	≤ 0.25	> 0.25
0	S/A				S/A	
0.125	S/A				S/A	
0.25	S/A				S/A	
0.375		S/A				
0.5		A	S			
0.625				S/A		

5.2. FAM validation for non-aggregated cross traffic scenarios

We use this section to validate the accuracy of our method FAM when we consider the models' outcomes based on aggregated and non-aggregated cross traffic. We here consider non-aggregated cross traffic scenarios. Analogously to the previous section, we validate the method by comparing its estimation to the results delivered by the network simulator.

Scenario #1 - Three STAs. We here evaluate FAM's accuracy when we used the scenario described in Figure 5, where an 802.11n WLAN and an 802.11g WLAN were deployed.

Table 6 shows that FAM estimates well the BTF and the type of the traffic for the cases 0, 0.25, 0.3.75, 0.5 and 0.625 and overestimates the BTF for the case BTF=0.125. Unfortunately, the Wi-Fi link may experience several transient effects in practice. Since the analytical model neglects some protocol aspects such as beacons and MAC losses, it underestimates the aggregation level for some probe packet gaps. As a result, FAM overestimates the BTF which is typically a better outcome for most applications than an aggressive underestimate.

Table 6: BTF and cross traffic nature estimations for ns3 simulations, non-aggregated cross traffic - Three STAs

Ground Truth BTF	Estimated BTF and cross traffic nature					
	Cross traffic aggregates				Cross traffic does not aggregate	
	≤ 0.25	0.375	0.5	0.625	≤ 0.25	> 0.25
0	S/A				S/A	
0.125	S	A			S	
0.25	S/A				S/A	
0.375						S/A
0.5						S/A
0.625						S/A

Scenario #2 - Six STAs. We now consider the case where we vary the number of cross traffic nodes from one to four.

Table 7 shows the corresponding results. The results of four cross traffic STAs show similar tendencies to the results with a single cross traffic STA. Based on these results, we can observe that FAM finds the same results as the previous case. In summary, we find that our method provides relative errors generally smaller than 10%.

Table 7: BTF and cross traffic nature estimations for ns3 simulations for the case where the cross traffic is non-aggregated - Six STAs

Ground Truth BTF	Estimated BTF and cross traffic nature					
	Cross traffic aggregates				Cross traffic does not aggregate	
	≤ 0.25	0.375	0.5	0.625	≤ 0.25	> 0.25
0	S/A				S/A	
0.125	S	A				
0.25	S/A				S/A	
0.375						S/A
0.5						S/A
0.625						S/A

6. Related work

Performance evaluation of Wi-Fi networks has been intensely studied in the literature to offer relevant information and methods to help its configuration and improvement. In this paper, we focus on three categories of work: Available bandwidth estimation, crowd-sensing of wireless networks, and Analytical models.

Available bandwidth estimation. Conversely to achievable throughput estimation tools, there exists another pivotal metric for estimating the overall network performance which is the available bandwidth. Active Available bandwidth measurements that involve the usage of probing packets can be generally divided into two categories: Packet Rate Model (PRM) and Probe Gap Model (PGM). The works based on PRM, such as TOPP [5], pathload [6], pathChirp [7] and DietTOPP [8], focus on comparing the probe packet and received packet rates. They inject increasing probe traffic in the network path and try to find the point where link congestion starts occurring to discern the available bandwidth. These methods differ according to the probing rate settlement.

Conversely to PRM, PGM techniques (e.g., Spruce [9], Initial Gap Increase/Packet Transmission Rate (IGI/PTR) [10], Delphi [11]...) leverage the dispersion in time between two received packets to infer the cross traffic. All these approaches were primitively focused on wired networks and unfortunately failed with the complexity of CSMA/CA of Wi-Fi networks. To copy with this latter, more complex schemes were developed, such as Exact [12], IdleGap [13] and WBest [14]. These techniques intensely depend on the fact that the received packet rate or packet gap should be an effective indicator to reveal the cross traffic. However, the dissimilar packet scheduling system under frame aggregation, proposed by modern Wi-Fi versions, prevents the use of these techniques as inter-packet arrival becomes null when they were embedded in the same aggregated frame. For monitoring the network conditions of these new versions of Wi-Fi, WBest+ [2] and AIWC [3] use the characteristics of frame aggregation to discern the available bandwidth by relying on a threshold-based method: if an inter-arrival time is less than a given threshold, the two packets are considered as aggregated. In [15], the mean aggregation level is compared to the one of an analytical model to estimate the network load. The network scenario used in these papers consists of a server with a wired Internet connection that sends [2, 3] or receives [15] probing traffic along the network path to/from a client with a last-hop wireless connection that assumed to be the bottleneck. The scenario considered here is different as both the probe traffic generator and the receiver are associated with the same Wi-Fi AP. The behavior of the mean aggregation is then much more complex as it may be different on the uplink and downlink links due to their different parameters (e.g., MCS). Moreover, the probe traffic accesses twice the channel that decreases the level of probe traffic for which the network becomes saturated and the size of the aggregated frames. While evaluating the probe aggregation levels of the UL probe traffic, the model presented in [15] assumes that the connection between the AP and the server is ideal. It is therefore modeled as if the server were implemented on the AP. However, the model presented here appraises the aggregation levels of the DL probe traffic by considering that the server is embedded on a second wireless device which is more realistic and practical.

Crowd-sensing. Alternatively, some techniques focus on crowd-sensing applications where mobile devices become active sensors to actively estimate the end-to-end network performance. The authors of [16] proposed MCNet, a tool

based on active smartphone measurements to estimate the user-perceived performance in enterprise wireless networks. Another work based on channel scans (spectrum sensing) was also proposed in [17]. It is based on passive measurements while our work investigate the effectiveness of active ones. The authors in [18] proposed a measurement crowd-sensing study in the city of Edinburgh to characterize urban Wi-Fi. It revealed several problems in Wi-Fi deployments in public spaces. However, none of these works involves the network load while crowd-sensing the network performance.

Analytical models. Wi-Fi Frame aggregation has attracted a lot of attention due to the significant efficiency enhancements brought by this feature. Consequently, several frame aggregation analytical models have been studied in recent years. [19, 20] predict throughput while incorporating frame aggregation under saturated conditions. A Discrete-Time Markov Chain (DTMC) that considers the frame aggregation has been proposed to show its performance under various aspects under unsaturated conditions [21]. Unfortunately, these models are not applicable or extensible to our work since they consider dissimilar scenarios and traffic patterns.

7. Conclusion

In this paper, we have proposed analytical models that predict the DownLink aggregation levels of a targeted probe traffic concurrent to cross traffic that can aggregate or not its frames. Based on that, we proposed a method that allows a vanilla device, in particular a smartphone, to estimate the expected network load via the Busy Time Fraction and infer if the current traffic aggregates its frames or not.

Our models and our method were validated through ns-3 simulations across a variety of scenarios.

Overall, from a general view point and for almost all the tested scenarios, we find that the models and the method estimate with a satisfactory degree of precision the aggregation levels of the probe traffic and the Busy Time Fraction respectively with at most 10% of errors. Based on six levels of network loads from to 0 to 0.625 with a resolution of 0.125, FAM seeks to classify the APs into three classes according to the network load: low, medium, and high loaded APs. It therefore compares APs with each others to detect the APs that are less loaded and provide guidance to hierarchize different WLANs. However, we should note that if an application needs better resolution, FAM can be adapted according to this new resolution.

Our future efforts include addressing some of the open challenges in network load estimation by an unmodified mobile device and the extension of the proposed method to be used in a crowd-sensing context.

References

[1] Cisco, Annual internet report (2018–2023) white paper (2020).

[2] A. Farshad, M. Lee, M. K. Marina, F. Garcia, On the impact of 802.11n frame aggregation on end-to-end available bandwidth estimation, in: IEEE International Conference on Sensing, Communication, and Networking (SECON), 2014, pp. 108–116. doi:10.1109/SAHCN.2014.6990333.

[3] L. Song, A. Striegel, Leveraging frame aggregation for estimating wifi available bandwidth, in: IEEE International Conference on Sensing, Communication, and Networking (SECON), 2017, pp. 1–9. doi:10.1109/SAHCN.2017.7964908.

[4] IEEE, Standard for information technology–telecommunications and information exchange between systems - local and metropolitan area networks–specific requirements - part 11: Wireless lan medium access control (mac) and physical layer (phy) specifications, IEEE Std 802.11-2020 (Revision of IEEE Std 802.11-2016) (2020) 1–4379doi:10.1109/IEEESTD.2021.9363693.

[5] B. Melander, M. Bjorkman, P. Gunningberg, A new end-to-end probing and analysis method for estimating bandwidth bottlenecks, in: IEEE Global Telecommunications Conference (Globecom), Vol. 1, 2000, pp. 415–420. doi:10.1109/GLOCOM.2000.892039.

[6] M. Jain, C. Dovrolis, Pathload: A Measurement Tool for End-to-End Available Bandwidth, in: Passive and Active Measurement Workshop (PAM), 2002, pp. 14–25.

[7] V. Ribeiro, R. Riedi, J. Navrátil, L. Cottrell, PathChirp: Efficient Available Bandwidth Estimation for Network Paths, in: Passive and Active Measurement Workshop (PAM), 2003, pp. 1–11. doi:10.2172/813038.

[8] A. Johnsson, M. Bjorkman, B. Melander, An Analysis of Active End-to-end Bandwidth Measurements in Wireless Networks, in: IEEE/IFIP Workshop on End-to-End Monitoring Techniques and Services, 2006, pp. 74–81. doi:10.1109/E2EMON.2006.1651282.

[9] J. Strauss, D. Katabi, F. Kaashoek, A measurement study of available bandwidth estimation tools, in: ACM SIGCOMM Conference on Internet Measurement (IMC), 2003, p. 39–44. doi:10.1145/948205.948211.

[10] N. Hu, P. Steenkiste, Evaluation and characterization of available bandwidth probing techniques, IEEE Journal on Selected Areas in Communications 21 (6) (2003) 879–894.

[11] V. Ribeiro, M. Coates, R. Riedi, S. Sarvotham, B. Hendricks, R. Baraniuk, Multifractal cross-traffic estimation, in: ITC Specialist Seminar on IP Traffic Measurement, Modeling, and Management, 2000, pp. 15–1.

[12] S. Shah, K. Chen, K. Nahrstedt, Available bandwidth estimation in ieee 802.11-based wireless networks, First ISMA/CAIDA Workshop on Bandwidth Estimation (BEst).

[13] H. K. Lee, V. Hall, K. H. Yum, K. I. Kim, E. J. Kim, Bandwidth estimation in wireless lans for multimedia streaming services, in: IEEE International Conference on Multimedia and Expo (ICME), 2006, pp. 1181–1184. doi:10.1109/ICME.2006.262747.

[14] M. Li, M. Claypool, R. Kinicki, Wbest: A bandwidth estimation tool for ieee 802.11 wireless networks, in: 2008 33rd IEEE Conference on Local Computer Networks (LCN), 2008, pp. 374–381. doi:10.1109/LCN.2008.4664193.

[15] N. E. H. Bouzouita, A. Busson, H. Rivano, Analytical study of frame aggregation level to infer IEEE 802.11 network load, in: International Wireless Communications and Mobile Computing (IWCMC), 2020, pp. 952–957. doi:10.1109/IWCMC48107.2020.9148448.

[16] S. Rosen, S. Lee, J. Lee, P. Congdon, Z. M. Mao, K. Burden, Mcnet: Crowdsourcing wireless performance measurements through the eyes of mobile devices, IEEE Communications Magazine 52 (10) (2014) 86–91. doi:10.1109/MCOM.2014.6917407.

[17] J. Shi, L. Meng, A. Striegel, C. Qiao, D. Koutsonikolas, G. Challen, A walk on the client side: Monitoring enterprise wifi networks using smartphone channel scans, in: IEEE International Conference on Computer Communications (IEEE INFOCOM), 2016, pp. 1–9. doi:10.1109/INFOCOM.2016.7524453.

[18] A. Farshad, M. K. Marina, F. Garcia, Urban wifi characterization via mobile crowdsensing, in: IEEE Network Operations and Management Symposium (NOMS), 2014, pp. 1–9. doi:10.1109/NOMS.2014.6838233.

[19] N. Mohammad, S. Muhammad, Modeling and analyzing mac frame aggregation techniques in 802.11n using bi-dimensional markovian model, Vol. 293, 2012, pp. 408–419. doi:10.1007/978-3-642-30507-8_35.

[20] N. Hajlaoui, I. Jabri, M. Ben Jemaa, An accurate two dimensional Markov chain model for IEEE 802.11n DCF, Wireless Networks 24 (2018) 1019–1031. doi:10.1007/s11276-016-1383-z.

[21] B. S. Kim, H. Y. Hwang, D. K. Sung, Effect of frame aggregation on the throughput performance of ieee 802.11n, in: IEEE Wireless Communications and Networking Conference (WCNC), 2008, pp. 1740–1744. doi:10.1109/WCNC.2008.310.

Appendix A. Frame transmission duration

In this paper, the frame transmission duration takes into account the data packet transmission itself and all protocol overheads (backoff, SIFS, DIFS and

ACK or block ACK transmission). The transmission duration of l sub-frames is expressed as :

$$T_{AP}(l) = T_{DIFS} + T_{backoff} + T_{PHY} + T_{SIFS} + T_{Block\ ACK} + \frac{1}{freq} \times T_{Block\ ACK\ Request} + \frac{(MPDU Delimiter + MacHeader + Payload + FCS) \times 8 \times l}{Physical\ transmission\ rate}$$

Where freq denotes the frequency of sending of block ACK requests. $T_{backoff}$ denotes the mean duration of the backoff period for frames without retransmissions. It is given by:

$$T_{backoff} = \frac{CW_{min}}{2} \times T_{slot}$$

$T_{BlockACK}$ and T_{ACK} denote respectively the time required to send the block acknowledgment frame and the acknowledgment frame. They also count their physical header.

Note that the only difference between the functions $T_{AP}(.)$ and $T_{AC}(.)$ is the physical transmission rate and the packet size that depend on the local properties of the nodes.

Appendix B. additional probabilities for the model based on aggregated cross traffic

$$\mathbb{P}\Big(S_{n+1} = APC | S_n = APP, Z_{n+1} = q, Y_{n+1} = m > 0\Big) = \frac{1}{2}\mathbb{1}_{q>0} + \mathbb{1}_{q=0}$$

$$\mathbb{P}\Big(S_{n+1} = SP | S_n = APP, Y_{n+1} = m, Z_{n+1} = q > 0\Big) = \frac{1}{2}\mathbb{1}_{m>0} + \mathbb{1}_{m=0}$$

$$\mathbb{P}\Big(S_{n+1} = APP | S_n = APC, X_{n+1} = X_n = l > 0, Z_{n+1} = q\Big) = \frac{1}{2}\mathbb{1}_{q>0} + \mathbb{1}_{q=0}$$

$$\mathbb{P}\Big(S_{n+1} = APC | S_n = APC, X_n = X_{n+1} = 0, Y_{n+1} = m > 0, Zn + 1 = q\Big) = \frac{1}{2}\mathbb{1}_{q>0} + \mathbb{1}_{q=0}$$

$$\mathbb{P}\Big(S_{n+1} = SP | S_n = APC, Z_{n+1} = q > 0, X_{n+1} = X_n = l, Y_{n+1} = m\Big) = \frac{1}{2}\mathbb{1}_{l+m>0} + \mathbb{1}_{l+m=0}$$

$$\mathbb{P}\Big(S_{n+1} = APP | S_n = SP, X_{n+1} = l > 0, Z_{n+1} = q, Y_{n+1} = l\Big) = \frac{1}{2} \cdot \frac{1}{2}\mathbb{1}_{q>0,m>0} + \frac{1}{2}\mathbb{1}_{q>0,m=0} + \frac{1}{2}\mathbb{1}_{q=0,m>0} + \mathbb{1}_{q=0,m=0}$$

$$\mathbb{P}\Big(S_{n+1} = APC | S_n = SP, Y_{n+1} = m > 0, Z_{n+1} = q, X_{n+1} = l\Big) = \frac{1}{2} \cdot \frac{1}{2}\mathbb{1}_{q>0,l>0} + \frac{1}{2}\mathbb{1}_{q>0,l=0} + \frac{1}{2}\mathbb{1}_{q=0,l>0} + \mathbb{1}_{q=0,l=0}$$

$$\mathbb{P}\Big(S_{n+1} = SP | S_n = SP, Z_{n+1} = q > 0, X_{n+1} = l, Y_{n+1} = m\Big) = \frac{1}{2}\mathbb{1}_{m+l>0} + \mathbb{1}_{m+l=0}$$

Appendix C. additional probabilities for the model based on non-aggregated cross traffic

$$\mathbb{P}\Big(S_{n+1} = APC | S_n = APP, X_{n+1} = l = 0, Y_{n+1} = m > 0, Z_{n+1} = q\Big) = \frac{1}{2}\mathbb{1}_{q>0} + \mathbb{1}_{q=0}$$

$$\mathbb{P}\Big(S_{n+1} = SP | S_n = APP, X_{n+1} = l = 0, Y_{n+1} = m, Z_{n+1} = q > 0\Big) = \frac{1}{2}\mathbb{1}_{m>0} + \mathbb{1}_{m=0}$$

$$\mathbb{P}\Big(S_{n+1} = APC | S_n = APC, X_n = X_{n+1} = i = l, Y_{n+1} = m > 0, Z_{n+1} = q\Big) = \frac{1}{3}\mathbb{1}_{q>0,l>0} + \frac{1}{2}\mathbb{1}_{q>0,l=0} + \frac{1}{2}\mathbb{1}_{q=0,l>0} + \mathbb{1}_{q=0,l=0}$$

$$\mathbb{P}\Big(S_{n+1} = APP | S_n = APC, X_{n+1} = X_n = i = l > 0, Y_{n+1} = m, Z_{n+1} = q\Big) = \frac{1}{3}\mathbb{1}_{q>0,m>0} + \frac{1}{2}\mathbb{1}_{q>0,m=0} + \frac{1}{2}\mathbb{1}_{q=0,m>0} + \mathbb{1}_{q=0,m=0}$$

$$\mathbb{P}\Big(S_{n+1} = SP | S_n = APC, Z_{n+1} = q > 0, X_{n+1} = X_n = i = l, Y_{n+1} = m, Z_{n+1} = q > 0\Big) = \frac{1}{3}\mathbb{1}_{l>0,m>0} + \frac{1}{2}\mathbb{1}_{l>0,m=0} + \frac{1}{2}\mathbb{1}_{l=0,m>0} + \mathbb{1}_{l=0,m=0}$$

$$\mathbb{P}\Big(S_{n+1} = APP | S_n = SP, X_{n+1} = l > 0, Y_{n+1} = m, Z_{n+1} = q\Big) = \frac{1}{3}\mathbb{1}_{q>0,m>0} + \frac{1}{2}\mathbb{1}_{q>0,m=0} + \frac{1}{2}\mathbb{1}_{q=0,m>0} + \mathbb{1}_{q=0,m=0}$$

$$\mathbb{P}\Big(S_{n+1} = APC | S_n = SP, X_{n+1} = l, Y_{n+1} = m > 0, Z_{n+1} = q\Big) = \frac{1}{3}\mathbb{1}_{q>0,l>0} + \frac{1}{2}\mathbb{1}_{q>0,l=0} + \frac{1}{2}\mathbb{1}_{q=0,l>0} + \mathbb{1}_{q=0,l=0}$$

$$\mathbb{P}\Big(S_{n+1} = SP | S_n = SP, X_{n+1} = l, Y_{n+1} = m, Z_{n+1} = q > 0\Big) = \frac{1}{3}\mathbb{1}_{l>0,m>0} + \frac{1}{2}\mathbb{1}_{l>0,m=0} + \frac{1}{2}\mathbb{1}_{l=0,m>0} + \mathbb{1}_{l=0,m=0}$$